Electrified, decentralised upcycling of Platinum-Group Metals from spent automotive catalysts into functional electrocatalysts

– Supplementary information

Luis F. Leon-Fernandez[1,†,*], *Frantisek Kukurugya* [1], *Omar Martinez-Mora*[1,2], *Stefanos Mourdikoudis*[1,‡], *Lunjie Zeng*[3], *Maria M. Parascanu*[4], *Aitana Saez*[4], *Jan Fransaer*[2], *Jeroen Spooren*[1], *Xochitl Dominguez-Benetton*[1,§,*]

[1] Material and Chemistry Unit (MatCh), Flemish Institute for Technological Research (VITO), Boeretang 200, 2400, Mol, Belgium.

[2] Department of Materials Engineering, Surface and Interface Engineered Materials, Katholieke Universiteit Leuven, Kasteelpark Arenberg 44 - box 2450, 3001 Leuven, Belgium.

[3] Department of Physics, Chalmers University of Technology, 41296 Göteborg, Sweden

[4] TECNALIA, Basque Research and Technology Alliance (BRTA), Astondo Bidea, Edificio 700, Derio, 48160, Spain

[†] *Current affiliation*: Applied Electrochemistry & Catalysis (ELCAT), University of Antwerp, Universiteitsplein 1, 2610, Wilrijk, Belgium

[‡] *Current affiliation*: CINBIO, Universidade de Vigo, Department of Physical Chemistry, Campus Universitario Lagoas Marcosende, Vigo, 36310 Spain

[§] *Current affiliation*: Equinor Energy Belgium, Kortenberglaan 120, 1000, Brussels, Belgium

1. ESI-I Basis and Sensitivity Analysis of Lost PGM Recovery Potential

For the EU alone, using the Commission's estimate of ~3.5 million 'missing' ELVs per year and conservative catalyst-loading assumptions, the unrealised secondary supply from missing vehicles alone is on the order of ~7–22 t PGM per year, equivalent to ~6–19% of EU total PGM demand (or ~8–24% of EU automotive PGM demand) in 2022.

Anchor facts:

1. EU "missing ELVs" = ~3.5 million per year (≈ one-third of deregistered vehicles)[1].
2. 2022 EU automotive PGM demand = ~2.956 million oz ≈ 92 t (Pt+Pd+Rh)[2].
3. 2022 EU total PGM demand (Pt+Pd) = ~111 t (Pt 40.5 t, Pd 70.7 t; Rh not regionally tabulated)[2].
4. 2022 global Rh demand = 31.3 t; using Europe's auto share (~24.2% of global auto PGM demand) gives EU Rh ≈ 7–8 t[2].

Estimate of unrealised EU secondary supply from "missing ELVs" (7–22 t range):

- As a share of EU total PGM demand (~119 t in 2022, Pt+Pd+Rh) → ~6–19%.
- As a share of EU automotive PGM demand (~92 t) → ~8–24%[2].

Given that automotive catalysts dominate PGM use and considering ELV leakage (often greater outside the EU) alongside low recovery from non-automotive streams, a conservative unrealised recovery opportunity is ~10–20% of annual PGM demand.

[1] European Commission. End-of-life vehicles regulation | Environment — European Commission. https://environment.ec.europa.eu/topics/waste-and-recycling/end-life-vehicles/end-life-vehicles-regulation_en (2025).

[2] Johnson Matthey. PGM Market Report May 2022. https://matthey.com/documents/161599/509428/PGM-market-report-May-2022.pdf (2022).

2. ESI-II MATERIALS AND METHODS

2.1. MWAL Analytical methods

The elemental composition of the investigated samples was analysed using inductively coupled plasma optical emission spectroscopy (ICP-OES). Prior to ICP-OES analyses, solid samples underwent acid digestion. The specific acid digestion procedure was tailored to each sample based on the metals of interest and the sample's characteristics. For the automotive catalyst sample, for which Pt, Pd and Rh were the main elements to analyse, closed microwave oven digestion was performed using a mixture of $HCl/HNO_3/HBF_4/H_2O_2$ (v/v = 5/4/3/3). The acid digestion was followed by ICP-OES analysis (Optima 3000 DV, PerkinElmer). Liquid samples were analysed exclusively by ICP-OES (Avio 500, PerkinElmer).

The mineralogical compositions of the initial samples were determined using powder X-ray diffraction (XRD) analysis. The XRD measurements were performed using a PANalytical Empyrean system (manufactured by PANalytical B.V. in Almelo, The Netherlands). The instrument was operated at 40 kV and 45 mA and equipped with a Co tube (1.7903 Å wavelength). Continuous XRD scans were conducted in a 2θ range of 5 to 120°. The resulting diffractograms were qualitatively analysed using HighScore Plus software to determine the mineralogical components present in the sample.

Particle size analyses were conducted using a vibratory sieve shaker (Model AS 200, Retsch, Germany). A set of sieves with specific pore sizes (1 mm and 0.5 mm) were assembled in a sieve stack for the analysis. The samples underwent sieving, and the resulting size fractions were collected and weighed. The finest fraction (< 0.5 mm) underwent additional analysis using a laser diffraction analyser (Partica mini LA-350, Horiba).

2.2. GDEx EXTENDED METHODOLOGY

2.2.1. Electrochemical cell operation

The general scheme of the three-compartment electrochemical reactor is depicted in Figure S1a. The general mechanism of the GDEx process for the precipitation of PGM NPs is presented in Figure S1b. The operating conditions are summarized in Table S1.

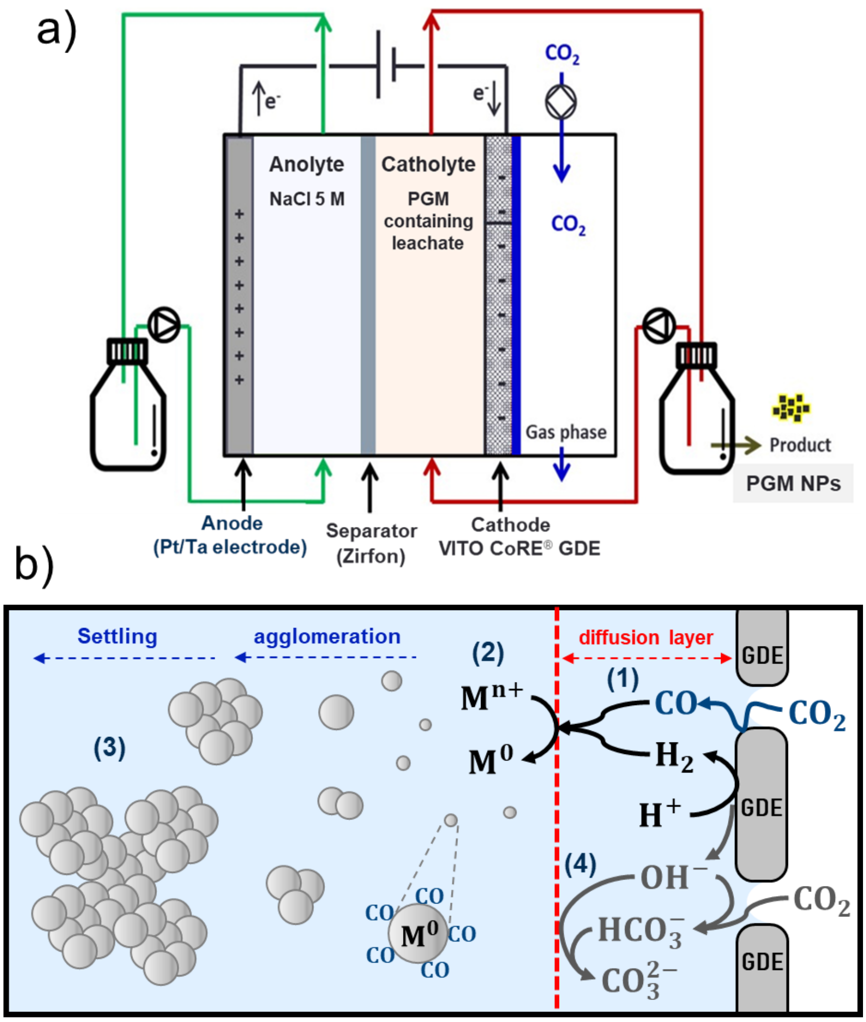

Figure S1. a) General scheme of the GDEx reaction b) General GDEx mechanism for the precipitation of PGM NPs at the cathode: (1) The CO_2 reduction reaction leads to the formation of CO, and the simultaneous water electrolysis to H_2; (2) CO and H_2 react with the metal ions in solution, where CO also acts as a size limiting agent; (3) this leads to the formation of metal nanoparticles, which agglomerate and settle. (4) Electrochemically unreacted CO_2 may dissolve and undergo equilibrium reactions, buffering the pH rise, yielding bicarbonate or carbonate depending on the medium pH.

Table S1. Operating conditions in GDEx tests.

Catholyte (100 mL)	Leachates from MWAL (pH < 0) Conductivity ~ 450 mS cm^{-1}
Anolyte (250 mL)	NaCl 5 M
Cathode	VITO CoRE® GDE
Anode	Pt/Ta electrode
Current density	-10 to -200 mA cm^{-2}
Electrode surface area	10 cm^2
Temperature	20–22 °C
Electrolyte flow rate	100 mL min^{-1}
Gas Flow rate	200 mL min^{-1}
Gas overpressure	20 mbar(g)
Reference electrode	Ag/AgCl (KCl 3M)

2.2.2. Gas flow regime

Two gas flow regimes were studied, the so-called flow-by (FB) and flow-through (FT) as illustrated in Figure S2. Under FB regime (Figure S2a), CO_2 was fed to the gas compartment with an overpressure of 20 mbar(g) and a flow rate of 200 mL min^{-1}. Under this regime, CO_2 flux from the gas chamber to the catholyte is driven by diffusion. Under FT conditions (Figure S2b) the outlet of the gas chamber was closed, and the flow rate was set at 5 mL min^{-1}. In this latter case, the CO_2 gas is thus forced to pass through the GDE, and therefore convective flow prevails in the system. When operating under gas FT regime, gas bubbles could be seen coming out of the GDE, both under electrochemical operation and at open circuit potential (OCP) conditions.

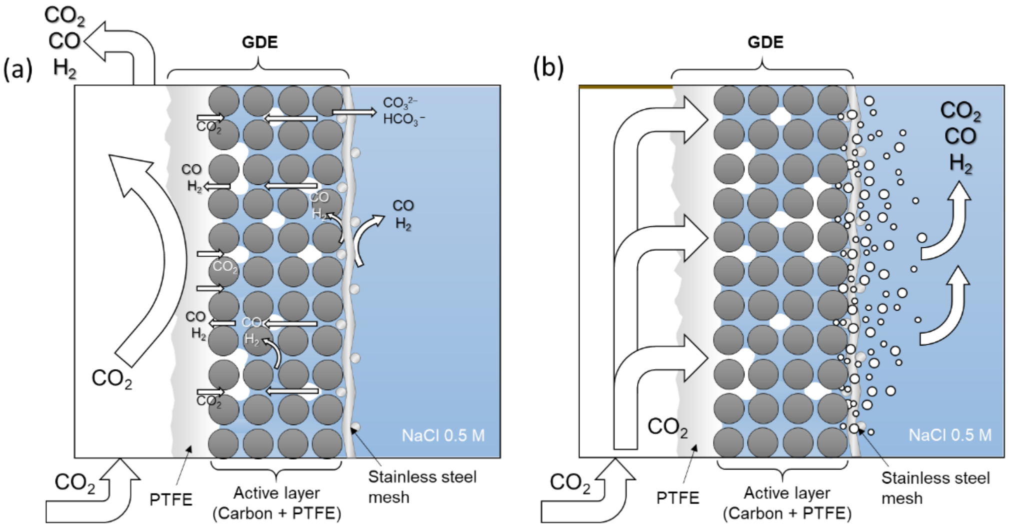

Figure S2. Different gas flow regimes investigated: (a) flow-by (FB) and (b) flow-through (FT).

2.2.3. Characterisation Methods

X-ray diffraction (XRD): The dried samples were analysed by XRD in a PANalytical Empyrean diffractometer operated at a voltage of 40 kV and a current of 45 mA using a Co Kα radiation source ($\lambda = 1.7903$ Å). Measurements were performed with 4 s per step and a step size of 0.05° 2θ in the 20°–120° 2θ range. Profile fitting of the powder diffraction patterns was performed with Highscore Plus (Malvern Panalytical) using the Inorganic Crystal Structure Database (ICSD).

Scanning Electron Microscopy (SEM): Micrographs of the dry samples were taken with a Philips XL30 FEG scanning electron microscope; images presented were recorded with secondary electrons and an acceleration voltage of 30 kV. The samples were prepared by dispersing the powders in ethanol and sonicating them for 30 min. Then, 10 µL were dropped onto an aluminium foil mounted on a sample holder. The mean particle size and particle size distribution were evaluated by counting at least 100 particles using ImageJ software (National Institutes of Health, Bethesda, MD, USA, version 1.53t, https://imagej.net/ij/) . After that, data were fitted to a lognormal distribution to obtain the mean particle size and standard deviation.

Transmission Electron Microscopy (TEM): A FEI Titan 80-300 TEM, operated at 300 kV, was used for bright field (BF) TEM imaging, and a JEOL monochromated ARM200F, equipped with probe Cs corrector and double SDD EDXS detector, was employed for STEM imaging and EDXS analysis. EDXS maps were obtained by integrating the intensity in the corresponding EDXS peaks from each element. The peaks used for mapping were manually selected to avoid overlapping between Rh-L and Pd-L, as well as Pt-M. The samples were prepared by dispersing the powders in distilled water. The dispersion was then drop-casted on a Cu TEM grid covered with holey carbon film. The grid was dried in ambient conditions for 15 min before being put in the TEM for measurements.

2.3. Assessment of the recovered PGM NPs as electrocatalysts for the Methanol Oxidation Reaction (MOR)

The electrocatalytic activity of the different recovered PGM NPs was assessed using a three-electrode setup on a Bio-Logic (VMP3) multichannel potentiostat. A Pt coil (~3.6 cm^2) was used as a counter electrode, along with an Ag/AgCl (3 M KCl) electrode as a reference electrode. A glassy carbon electrode (GCE, 3.0 mm diameter) was utilized as the working electrode. Before use, the GCE was polished with Al_2O_3 (0.05 µm) and rinsed with Millipore Milli-Q® water. The potentials measured against the Ag/AgCl electrode ($E_{Ag/AgCl}$) were converted to values against the reversible hydrogen electrode (RHE) (E_{RHE}) using the equation $E_{RHE} = E_{Ag/AgCl} + 0.059pH + E^0_{Ag/AgCl}$, where $E^0_{Ag/AgCl}$ is the potential of the Ag/AgCl (KCl 3 M) electrode *vs*. RHE (0.210 V).

To prepare the electrodes, 5 mg of each material was resuspended in water and sonicated for 30 minutes. 10 µL of the suspensions were deposited onto the GCE and left to dry at room temperature; the Pt loading was controlled to be around 60-70 µg cm^{-2}. Following this, 5 µL of Nafion 0.5 wt% were added to the GCE and allowed to dry in air to ensure catalyst adhesion. First, the electrochemical surface area (ECSA) was calculated using the copper underpotential electrodeposition (CuUPD) method. Second, cyclic voltammetry (CV) was performed in Ar-saturated 0.5 M H_2SO_4 at a high scan rate (100 mV s^{-1}) from 0.05 to 1.05 V *vs.* RHE until the CV did not change (around 100 cycles), then a CV at a scan rate of 10 mV s^{-1} was performed. Subsequently, the electrodes were transferred to an Ar-saturated 0.5 M H_2SO_4 + 5 mM $CuSO_4$ solution. The CuUPD was performed at a fixed potential (0.360 V vs RHE) for 100 seconds, followed by a linear sweep voltammetry (LSV) scan from the fixed potential to the upper potential (1.05 V vs RHE) at 10 mV s^{-1}. The charge associated with copper stripping was calculated to determine the charges associated with any oxide growth. This was done by subtracting the charge obtained using the same conditions in 0.5 M H_2SO_4. A specific charge of 0.42 µC cm^{-2} was used to convert the coulombic charge to the surface area using the following formula:

$$\mathrm{ECSA} = \frac{\mathrm{Q_{CuUPD}} \times 100}{420\ \mu\mathrm{C\ cm^{-2}} \times \mathrm{L}} = \mathrm{m^2 g^{-1}} \quad (1)$$

where $\mathrm{Q_{CuUPD}}$ (µC) is the charge associated with copper stripping and L (µg) the Pt or total PGM loading.

For MOR activity, CVs were acquired at 50 mV s^{-1} from 0.03 V to 1.05 V vs RHE in Ar-saturated 0.5 M H_2SO_4 + 1.0 M methanol. The accelerated durability tests (ADT) were carried out using CVs for 1000 cycles at 50 mV s^{-1} at the same potential window. The results were normalised to the Pt or total PGM loading and ECSA, which were employed to determine the mass activity (MA) and specific activity (SA) according to the following formulae:

$$\mathrm{j_{MA}} = \text{Mass activity} = \frac{\mathrm{j_f} \times 1000}{L} = \text{mA mg}_{\text{Pt}}^{-1} \tag{2}$$

$$\mathrm{j_{SA}} = \text{Specific activity} = \frac{\mathrm{j_{MA}} \times 0.1}{\text{ECSA}} = \text{mA cm}^{-2} \tag{3}$$

where $\mathrm{J_f}$ is the measured current density at the peak potential.

2.4. Life-cycle assessment

Table S2. Life Cycle Inventory dataset for 1g of recovered PGM, Base case.

Environmental aspect	Qnt.	Unit	LCI dataset
Base case.L/S=5, 200 mA cm^{-2} and NaCl			
Milling			
Raw material			
Auto-catalyst Ceramic monoliths	0.39	kg	-
Energy consumption			
Electricity	0.037	kWh	Electricity, low voltage {RER} | market group for | Cut-off, U
Final output			
Auto-catalyst powder	0.39	kg	-
MWAL			
Raw material			
Auto-catalyst powder	0.39	kg	-
Ancillary/reactants			
Hydrochloric acid 37%	0.22	L	Stoichiometric calculation of 37% concentration based on dataset: Hydrochloric acid, without water, in 30% solution state {RER} | market for | Cut-off,U
Energy consumption			
Electricity	1	kWh	Electricity, low voltage {RER} | market group for | Cut-off, U
Waste			
Solid residue	0.53	kg	Inert waste, for final disposal {RoW} | treatment of inert waste, inert material landfill | Cut-off, U
Final output			
MWAL Leachate	**1.77**	**L**	-
GDEx			
Raw material			
MWAL leachate	1.77	L	-
Ancillary/reactants			
Sodium chloride	8.27E-5	kg	Sodium chloride, powder {GLO} | market for | Cut-off, U
CO_2 gas	3.28E-3	kg	Carbon dioxide, liquid {RER} | market for | Cut-off, U
Tap water	1.21	L	Tap water {RER} | market group for | Cut-off, U
Energy consumption			
Electricity	0.08	kWh	Electricity, low voltage {RER} | market group for | Cut-off, U
Waste/effluents/emissions			
Spent anolyte	0.71	L	Neutralization*
Supernatant	0.52	L	Neutralization + precipitation**
Cl_2 gas emission	9.28E-3	kg	Emissions to air – Chlorine
Spent CO_2 emission	1.22E-3	kg	Emissions to air – Carbon dioxide
Evaporated water	1.77E-5	kg	Emissions to air – water
Final output			
PGM-NP dry pellets	**1**	**g**	**-**

1 *A theoretical neutralization process with sodium hydroxide for the acid spent anolyte effluent (pH 0.5) has been modelled. No process energy has been included

2 ** A theoretical neutralization + precipitation process with sodium hydroxide for the acid supernatant effluent (pH 1) containing heavy metals has been modelled, based on stoichiometry of precipitation of bearing metals quantified by ICP-OES. No energy process has been included, and the resulting salts and metallic hydroxides sent to landfill.

2.5. Extended methodology Techno-Economic Assessment

The Weighted Average Cost of Capital (WACC) represents the average rate that a company is expected to pay to all its security holders to finance its assets. It is widely utilized as a hurdle rate in capital budgeting decisions. The WACC was calculated as follows:

$$\mathrm{WACC} = \left(\frac{E}{V}\right) \times Re + \left(\frac{D}{V}\right) \times Rd \times (1 - Tc) \tag{4}$$

where E represents the market value of equity, D the market value of debt, V the total market value of the company's financing (Equity + Debt), R_e is the cost of equity, R_d the pre-tax cost of debt, and T_c the corporate income tax rate (reflecting the tax deductibility of interest). The WACC calculation considers the relative weights of each component of the company's capital structure, reflecting the expected cost of new capital. WACC was estimated at 7%, derived from a 10% cost of equity (R_e), 5% cost of debt (R_d), a 50:50 debt–equity ratio (D/V = E/V = 0.5, with E and D the market values of equity and debt, and V = E + D), and a 25% corporate tax rate (T_c), representative of current EU levels ($\mathrm{WACC} = 0.5 \times 0.10 + 0.5 \times 0.05 \times (1 - 0.25) \approx 7\%$).

On the other hand, in financial analysis, the Net Present Value (NPV) is a key valuation metric that assesses the profitability of an investment or project. It represents the difference between the present value of cash inflows and the present value of cash outflows over the investment's lifetime. The NPV is calculated as follows:

$$\mathrm{NPV} = \sum \frac{R_t}{(1 + r)^t} - C_0 \tag{5}$$

Here, R_t is the net cash flow at time t, where t can range from 1 to n for the number of periods (being 10 years for the present TEA). C_0 is the initial investment cost, and r is the discount rate—which reflects the opportunity cost of the invested funds, the time value of money, and the risk associated with future cash flows. In a Techno-Economic Assessment (TEA) for a process that comprises the entirety of a company's operation, the discount rate r can be assumed to be the Weighted Average Cost of Capital (WACC). A positive NPV at this rate suggests that the process can generate value exceeding its cost of capital, indicating its financial feasibility.

The Operating Profit Margin—also known as Earnings Before Interest and Taxes (EBIT)—is calculated by subtracting operating expenses (such as wages, depreciation, and cost of goods sold) from gross revenue. The Operating Profit Margin is a profitability ratio that measures the percentage of revenue left over after all variable production costs have been paid. It measures a company's efficiency in generating profit from its core business operations, before considering the impact of financing and taxes.

$$\mathrm{EBIT} = \frac{Operating\ Income}{Revenue} \times 100 \tag{6}$$

The Return on Investment (ROI) is a performance measure used to evaluate the efficiency or profitability of an investment. ROI is expressed as a percentage and is calculated using the formula:

$$\mathrm{ROI} = \frac{Net\ Profit}{Investment\ Cost} \times 100 \tag{7}$$

where the *Net Profit* is the gain from the investment minus the cost of the investment and *Investment Cost* is the initial amount of money invested.

3. ESI-III THERMODYNAMIC REACTIONS AND EQUATIONS FOR GDEx

This section outlines the key electrochemical and chemical reactions involved in the GDEx process for reducing platinum group metal (PGM) complexes. These reactions form the basis for the mechanistic interpretation of PGM nanoparticle formation described in the main text.

- Electrochemical reactions at the cathode (standard conditions):

$$CO_2 + 2H^+ + 2e^- \rightleftharpoons CO + H_2O \qquad E^0 = -0.106\ \text{V vs. SHE} \tag{8}$$

$$2H^+ + 2e^- \rightleftharpoons H_2 \qquad E^0 = 0\ \text{V vs. SHE} \tag{9}$$

- Reduction of metal complexes by H_2 and/or CO:

$$[PtCl_6]^{2-} + H_2 \rightarrow [PtCl_4]^{2-} + 2H^+ + 2Cl^- \qquad \Delta G^0 = -131.2\ \text{kJ mol}^{-1} \tag{10}$$

$$[PtCl_4]^{2-} + H_2 \rightarrow Pt^0 + 2H^+ + 4Cl^- \qquad \Delta G^0 = -145.7\ \text{kJ mol}^{-1} \tag{11}$$

$$[PdCl_4]^{2-} + H_2 \rightarrow Pd^0 + 2H^+ + 4Cl^- \qquad \Delta G^0 = -144.0\ \text{kJ mol}^{-1} \tag{12}$$

$$[PdCl_4]^{2-} + CO + H_2O \rightarrow Pd^0 + CO_2 + 2H^+ + 4Cl^- \qquad \Delta G^0 = -92.8\ \text{kJ mol}^{-1} \tag{13}$$

$$2[RhCl_6]^{3-} + 3H_2 \rightarrow 2Rh^0 + 6H^+ + 12Cl^- \qquad \Delta G^0 = -124.8\ \text{kJ mol}^{-1} \tag{14}$$

- Buffering reactions in the catholyte:

$$CO_2 + OH^- \rightleftharpoons HCO_3^- \qquad pK_a = 5.86\ \text{(in 0.5 M NaCl)} \tag{15}$$

$$HCO_3^- + OH^- \rightleftharpoons CO_3^{2-} + H_2O \qquad pK_a = 8.92\ \text{(in 0.5 M NaCl)} \tag{16}$$

4. ESI-IV SUPPLEMENTARY RESULTS

4.1 MWAL

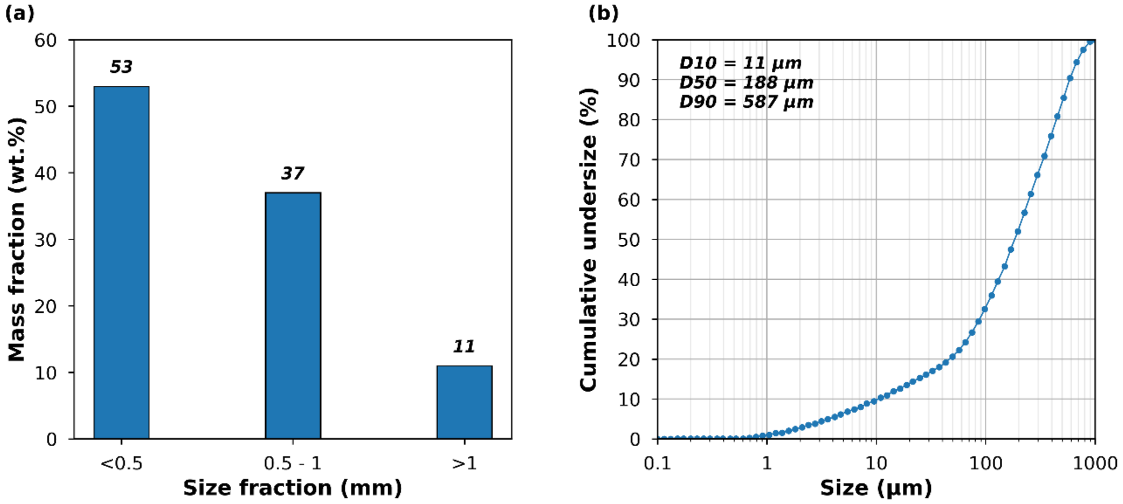

Figure S3. Particle size distribution of the spent automotive catalyst sample. (a) Mass fraction obtained by sieving into three size classes: <0.5 mm, 0.5–1 mm, and >1 mm. (b) Cumulative undersize distribution of the <0.5 mm fraction measured by laser diffraction, with characteristic particle diameters D10 = 11 µm, D50 = 188 µm, and D90 = 587 µm.

Table S3. Chemical composition of the spent automotive catalyst used in this study, in mg kg^{-1}.

Al	As	Ba	Ca	Ce	Co	Cr	Cu	Fe	La	Mg	Mn	Mo	Na	Nd	Ni	Pb	Pd	Pt	Rh	Si	Sr	Ti	V	Y	Zn	Zr
57168	221	695	3547	16516	-	213	126	3874	2421	8853	129	42	473147	642	232	368	1700	943	**272**	3632	1684	179	21	11	1874	-

Table S4. Composition of the L/S=10 - 6 M HCl leaching solution from the spent automotive catalyst, in mg L^{-1}.

	pH	Cond / mS cm^{-1}	ORP / mV	Al	As	Ba	Ca	Ce	Co	Cr	Cu	Fe	La	Mg	Mn	Mo	Na	Nd	Ni	Pb	Pd	Pt	Rh	Si	Sr	Ti	V	Y	Zn	Zr
Value	**-0.92**	**250**	**581**	**11161**	**26.4**	**207**	**357**	**2487**	**0.51**	**23.5**	**12.7**	**508**	**306**	**2816**	**16.2**	**9.4**	**104**	**106**	**25.7**	**38.3**	**163.8**	**95.2**	**29.2**	**74**	**174**	**99**	**3.0**	**3.3**	**204**	**<0.2**
SD	0.10	-	38	*5284*	*0.9*	*47*	*7*	*423*	*0.1*	*3.3*	*1.0*	*115*	*25*	*1737*	*3.1*	*0.5*	*24*	*12*	*7.3*	*1.6*	*5.3*	*6.0*	*3.4*	*6*	*7*	*47*	*1.2*	*1.5*	*36*	-

Table S5. Composition of the L/S=10 - 1.5 M NaCl, 1.5 M HCl leaching solution from the spent automotive catalyst, in mg L^{-1}.

	pH	Cond / mS cm^{-1}	ORP / mV	Al	As	Ba	Ca	Ce	Co	Cr	Cu	Fe	La	Mg	Mn	Mo	Na	Nd	Ni	Pb	Pd	Pt	Rh	Si	Sr	Ti	V	Y	Zn	Zr
Value	**-0.13**	**250**	**581.5**	**5431**	**21**	**66**	**337**	**1569**	**<0.5**	**20.2**	**12.0**	**368**	**230**	**841**	**12.3**	**4**	**44949**	**61**	**22**	**35**	**155.3**	**84.5**	**22.9**	**345**	**160**	**17**	**2**	**1**	**178**	**<0.2**
SD	0.12	-	11	1911	2	23	8	151	-	3.7	0.3	28	14	235	1.6	0.5	1384	5	6	1	4.1	6.7	4.1	9	3	2	0.1	0.1	14	-

Table S6. Composition of the L/S=5, leaching composition: 1.5 M NaCl, 1.5 M HCl leaching solution from the spent automotive catalyst, in mg L^{-1}.

	pH	Cond / mS cm^{-1}	ORP / mV	Al	As	Ba	Ca	Ce	Co	Cr	Cu	Fe	La	Mg	Mn	Mo	Na	Nd	Ni	Pb	Pd	Pt	Rh	Si	Sr	Ti	V	Y	Zn	Zr
Value	**0.61**	**250**	**521**	10354	35	4.6	582	2643	0.8	57.4	21.7	580	418	1268	22.3	6.8	34700	105	96	57	268.0	170.0	49.8	314	283	4.1	2.7	1.9	329	0.5

4.2 GDEx

Table S7. Dissolution of the GDE mesh during treatment of 6 M HCl leachates. Dissolution of mesh metals as a function of the current density applied.

Leaching solution	Polarization	Treatment time/min	Dissolved mass* / mg				
			Fe	Ni	Cr	Mn	Mo
1.5 M NaCl + 1.5 M HCl	10 mA cm^{-2}	240	3.0	1.5	3.9	-	0.3
	40 mA cm^{-2}	120	11.0	2.1	3.5	0.1	-
	200 mA cm^{-2}	60	5.0	0.6	1.2	-	0.0
6 M HCl	10 mA cm^{-2}	240	384.0	56.9	104.3	6.2	10.7
	40 mA cm^{-2}	120	276.0	40.7	63.3	4.5	7.6
	200 mA cm^{-2}	60	85.0	18.8	24.3	1.5	2.3

*The dissolved mass was calculated by subtracting the final metal concentration from the initial concentration and multiplying it by the volume of the solution.

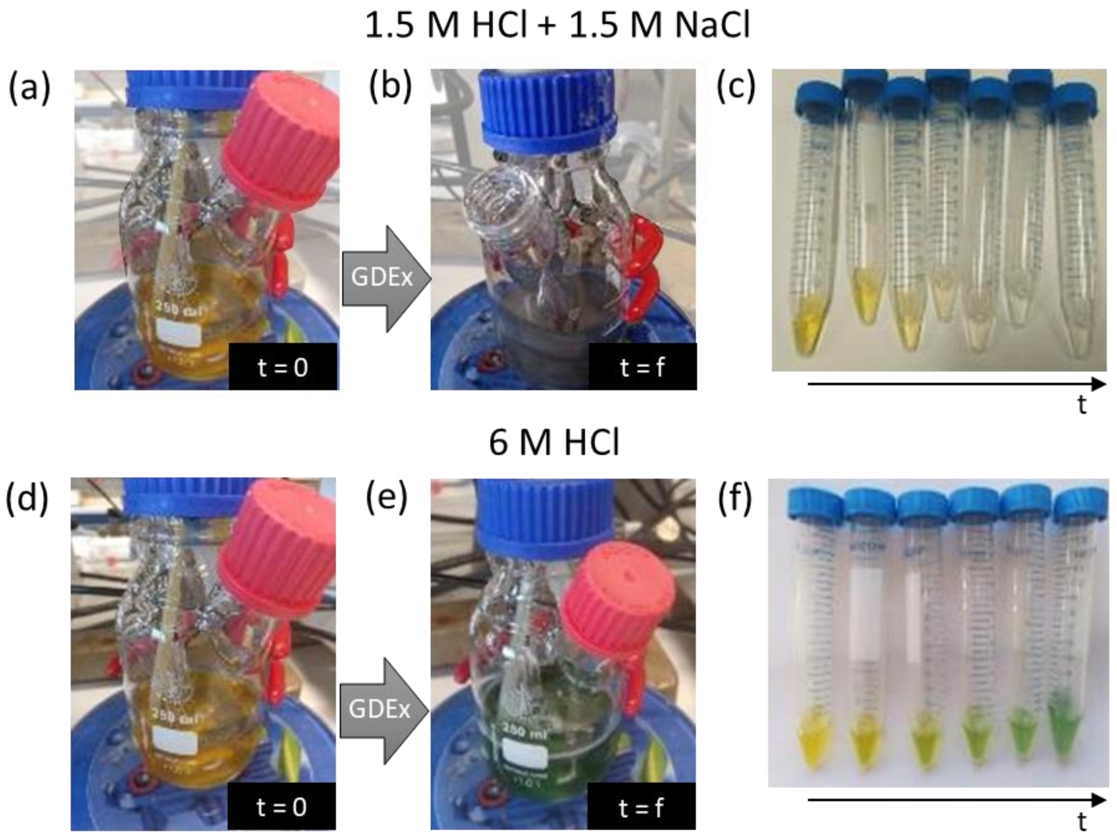

Figure S4. Visual representation of the evolution of the samples throughout the GDEx treatment. 1.5 M HCl + 1.5 M NaCl leachate solution (a) before and (b) after the GDEx process. (c) Evolution of the 1.5 M HCl + 1.5 NaCl leachate solution through time, the yellow color disappears as the PGMs are removed, and under conditions where the GDE mesh corrosion does not occur. 6 M HCl leachate solution (d) before and (e) after the GDEx process. (f) Evolution of the 6 M HCl leachate solution through time, the solution turned green due to the leaching of Fe and Ni ions from the GDE's stainless-steel mesh.

Table S8. Composition of the recovered MWAL-treated GDEx-nanoparticles (leaching solution: NaCl 1.5 M and HCl 1.5 M). The data are derived from the digestion of the particles and ICP-OES analysis.

	Metal content in the solid / % w/w		
Element	-10 mA cm^{-2}	-40 mA cm^{-2}	-200 mA cm^{-2}
Pd	49.2	48.1	54.3
Pt	28.0	28.2	30.5
Rh	7.1	7.1	6.3
Cu	3.8	2.7	1.8
Pb	9.3	8.9	5.4
Al	0.3	0.6	0.1
Others	2.7	5.1	1.6
PGM content (%)	84.2	83.3	91.2

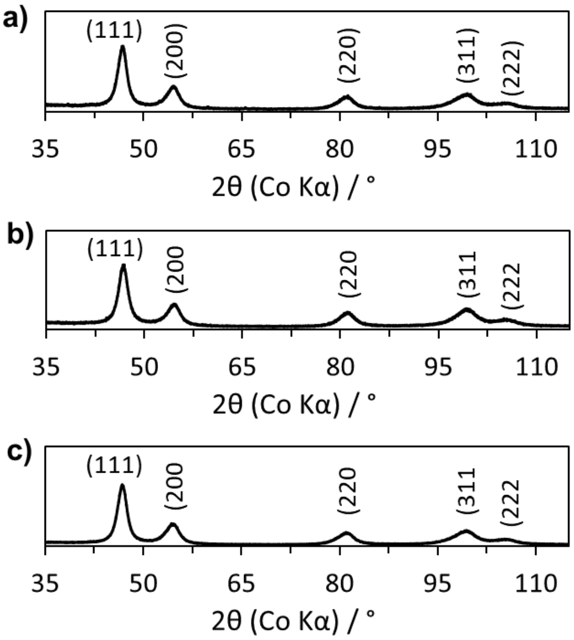

Figure S5. XRD spectra of the recovered solids after treating the 1.5 M HCl + 1.5 M NaCl leachate solutions with the GDEx process at a) 10 mA cm^{-2}, b) 40 mA cm^{-2} and c) 200 mA cm^{-2}.

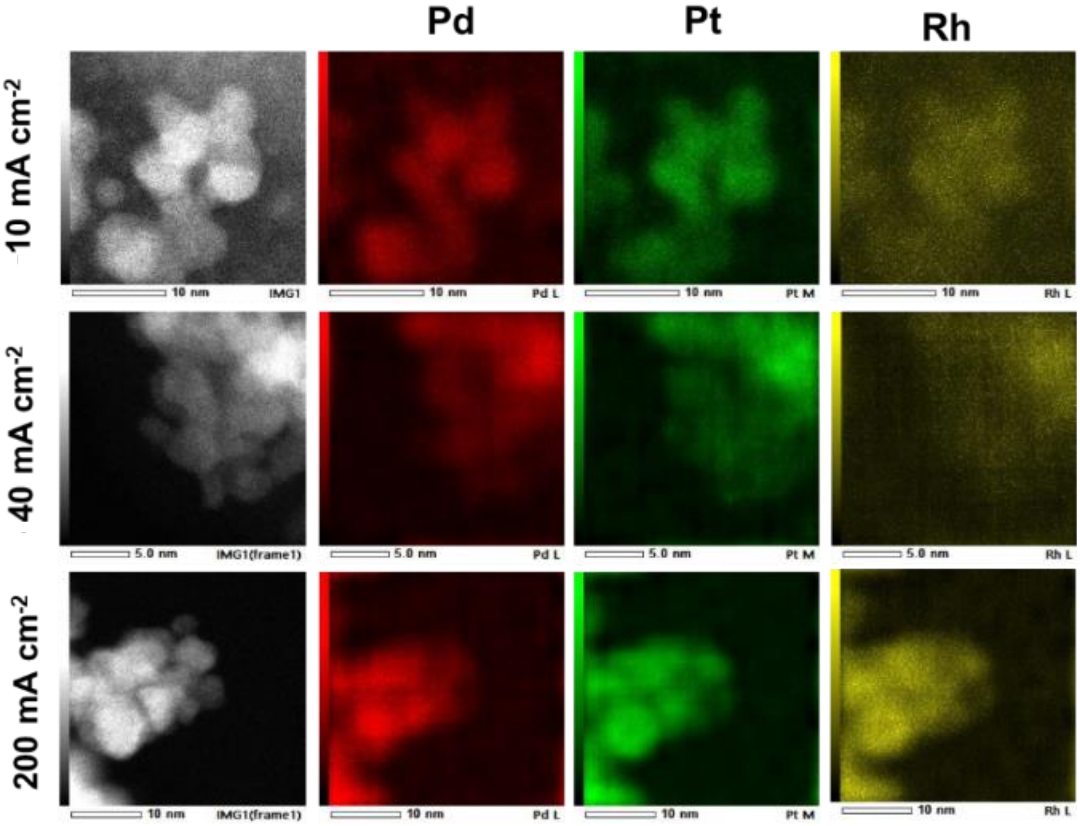

Figure S6. STEM-EDXS analysis of the products isolated after treating the 1.5 M HCl + 1.5 M NaCl leachate solutions with the GDEx process. Pd, Pt, and Rh are homogeneously distributed throughout the 5 nm nanoparticles, indicating the formation of an alloy structure.

Table S9. PGM surface atomic composition of the products obtained after the treatment of the 1.5 M HCl + 1.5 M NaCl leachate solutions with the GDEx process. Quantitative data acquired from the STEM-EDXS analysis.

Sample	Atomic percentage (%)		
	Pd	Pt	Rh
10 mA cm^{-2}	70.28	16.44	13.28
40 mA cm^{-2}	71.72	20.49	7.79
200 mA cm^{-2}	34.18	41.45	24.37

Table S10. Preselected default GDEx operating conditions

Current density	-40 mA cm^{-2}
Gas flow regime	Flow by
CO_2 gas flow rate	200 mL min^{-1}
Catholyte volume	100 mL
Anolyte volume	250 mL
Electrolyte recirculation flow rate	100 mL min^{-1}
Gas diffusion electrode	VITO-CoRE® (stainless steel mesh)
MWAL L/S ratio	L/S=10
MWAL composition	NaCl: 1.5 M HCl: 1.5 M

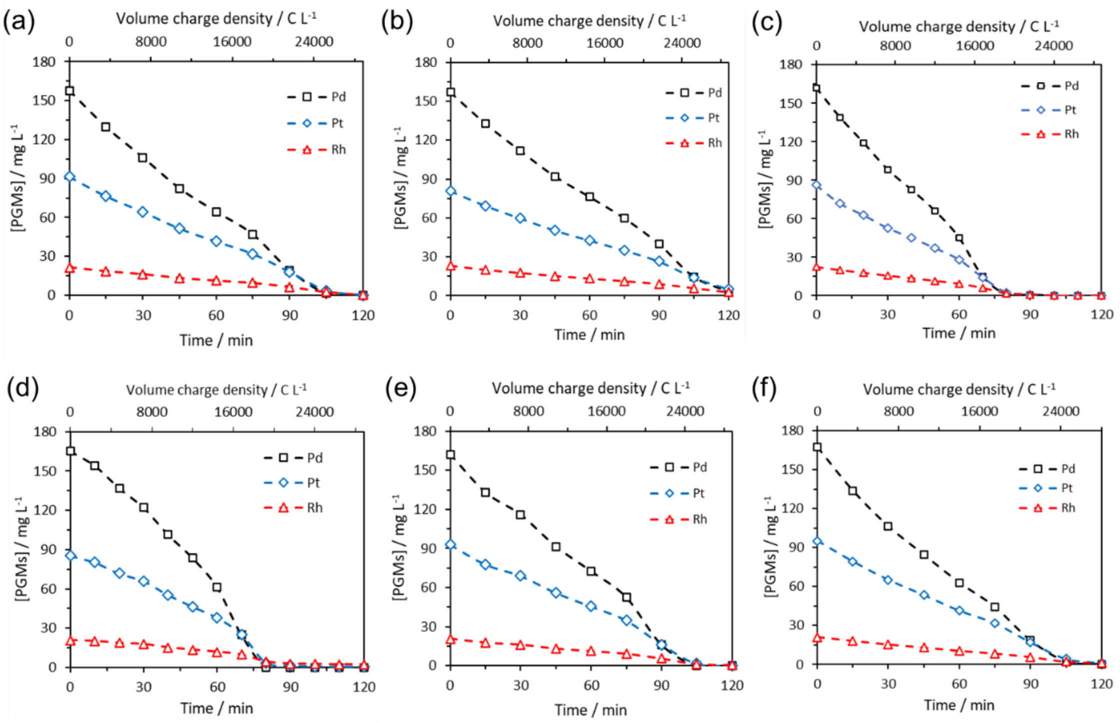

Figure S7. Comparison of experiments at 40 mA cm^{-2} and different parameters (100 mL solution). (a) Default conditions (200 mL min^{-1}, flow-by, VITO-CoRE® GDE, no sonication); (b) gas flow rate of 20 mL min^{-1}, flow-by; (c) flow-through regime (CO_2 gas flow rate of 5 mL min^{-1}); (d) sonication in recirculation tank; (e) anolyte used is Na_2SO_4, (f) Ti mesh in GDE.

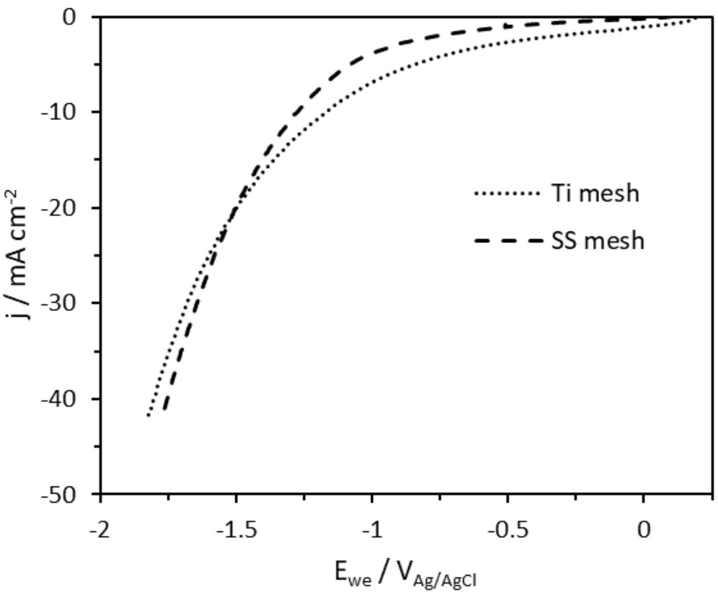

Figure S8. Linear Sweep Voltammograms were performed on meshes of different materials: SS mesh (used in the original VITO-CoRE® design) and black titanium mesh. The mesh size was 32 (Tyler Equivalent Mesh), with a window size of approximately 500 µm. The geometrical area of the tested meshes was 10 cm^2.

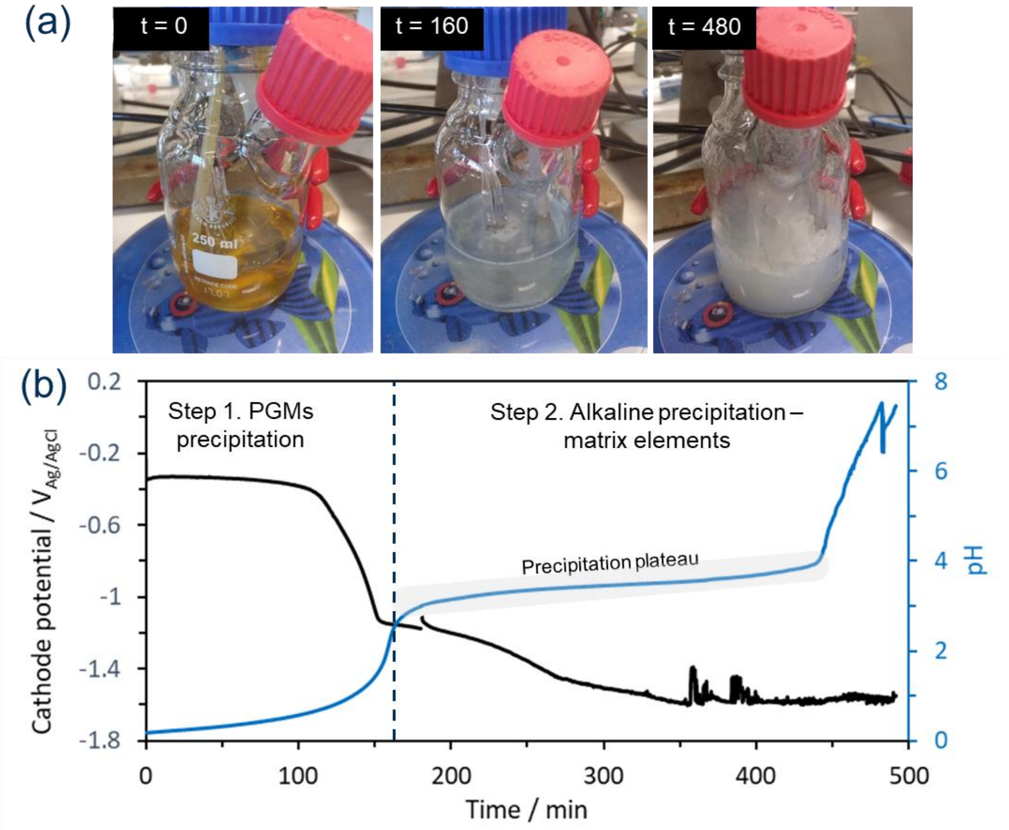

Figure S9. Treatment of automotive catalyst leachate (initial leaching solution: 1.5 M HCl + 1.5 M NaCl, L/S=10). (a) Appearance of the leachate at t = 0 when no precipitation had occurred (yellow color is due to the PGM ions presence), up to t = 160 min the precipitation of the PGMs took place (transparent solution with PGM particles in suspension), and after t = 160, when pH exceeded 2, precipitation of the matrix elements occurred, with a jelly texture and high viscosity, primarily due to aluminum and silicon (hydr)oxides. (b) Evolution of cathode potential and pH vs time, displaying pH plateau at pH > 2, when the alkaline precipitation of matrix elements occurred.

Table S11. Precipitation yield of metals after step 1 (t = 160 min) and step 2 (t = 490 min)

Precipitation yield (%)	**Rh**	**Pd**	**Pt**	Cu	Pb	Si	Ti	V	Mo	Al	Ce	Cr	Fe	La	Mn	Nd	Ni
Step 1	**99.3**	**99.2**	**99.5**	95.8	94.4	-	-	-	-	-	-	-	-	-	-	-	-
Step 2	-	-	-	100	100	100	100	100	100	100	99.9	98.1	94.4	99.2	100	100	89.7

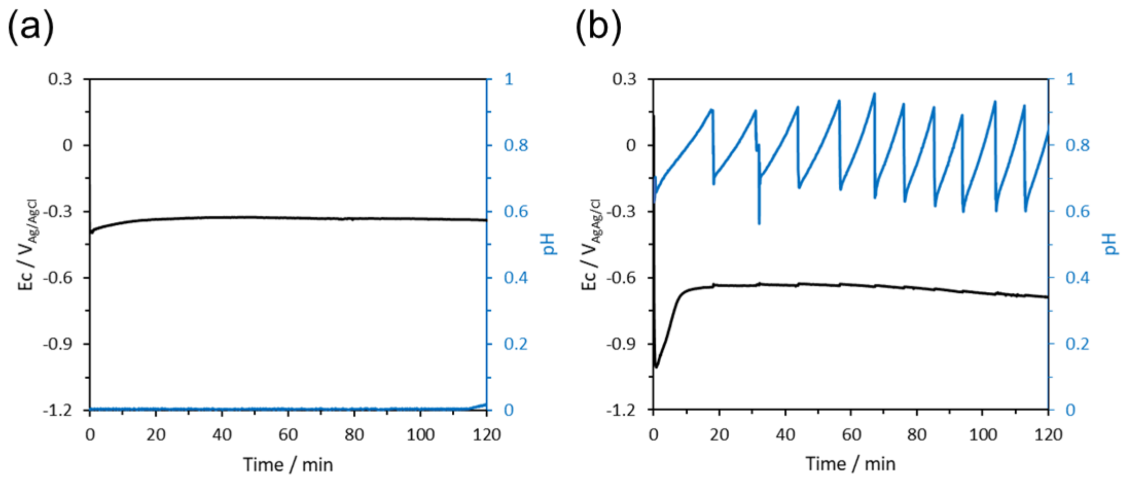

Figure S10. Cathode potential and pH evolution of the different MWAL samples during their treatment with GDEx. (a) L/S = 10, (b) L/S = 5. In (b), continuous acidification was applied to keep pH below 1 (see sawtooth pattern in the pH profile resulting from periodic 36% HCl aliquot additions).

4.3 Assessment of the recovered PGM NPs as electrocatalysts for the Methanol Oxidation Reaction (MOR)

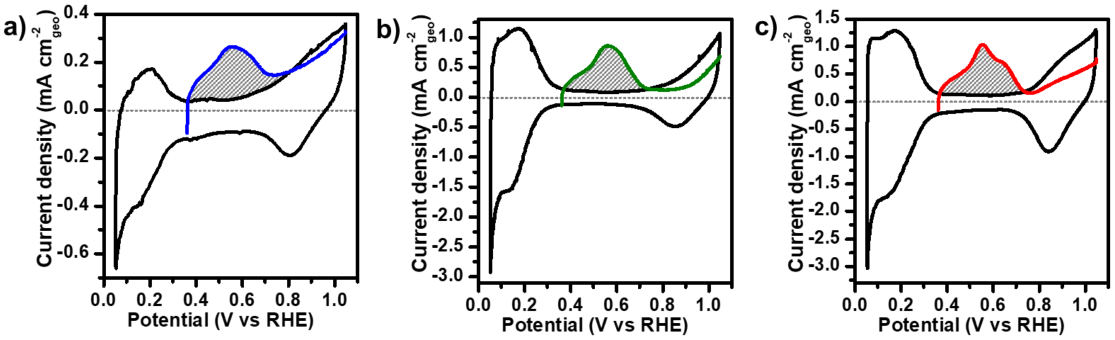

Figure S11. Background (black) and CuUPD stripping voltammetry (colour) for the PGM NPs recovered with GDEx at a) 10 mA cm^{-2}, b) 40 mA cm^{-2}, c) 200 mA cm^{-2}. The UPD stripping curves were obtained in 0.5 M H_2SO_4 and 5 mM $CuSO_4$, with the copper adsorbed at 0.360 V for 100 s. Background scans were performed in 0.5 M H_2SO_4. In all cases, the scan rate was 10 mV s^{-1}.

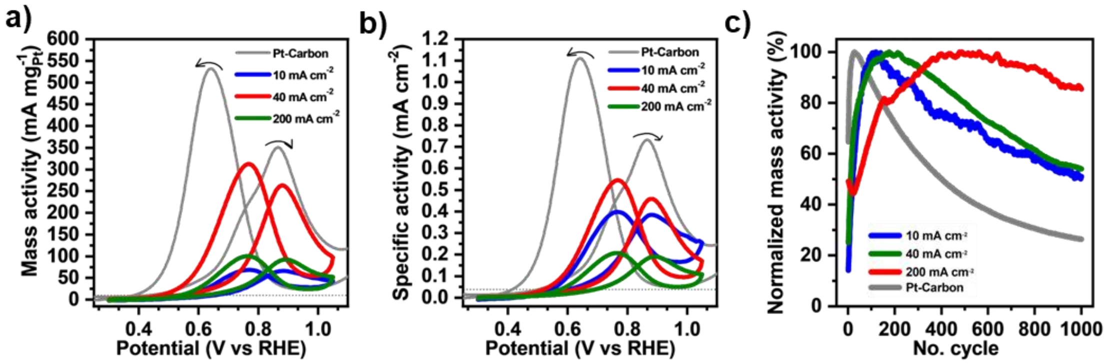

Figure S12**.** Electrocatalytic performance of the PGM nanoparticles recovered with GDEx towards the methanol oxidation reaction. a) Mass activity normalised to the Pt content, b) Specific activity normalised to ECSA, and c) Accelerated durability. The CVs were recorded in 0.5 M H_2SO_4 + 1.0 M methanol solution at 50 mV s^{-1}.

4.4 Life cycle assessment

Table S12. Characterised Environmental Impacts by Process Stage (Base Case: L/S=5, -200 mA cm^{-2} and 1.5 M NaCl)

Impact category	Unit	Milling	MWAL	GDEx	Total	Standard deviation	Coeff. of variation
CC	kg CO_2 eq	1.22E-02	4.57E-01	1.10E-01	5.79E-01	0.0259	4.47%
OD	kg CFC11 eq	2.28E-10	1.18E-08	4.55E-09	1.66E-08	3.66E-09	22.10%
POF	kg NMVOC eq	3.16E-05	1.24E-03	3.08E-04	1.58E-03	1.27E-04	8.06%
PMF	disease incidence	2.49E-10	1.14E-08	4.21E-09	1.59E-08	2.51E-09	15.80%
HTnc	CTUh	1.90E-10	6.80E-09	1.66E-09	8.65E-09	5.26E-07	1340%
HTc	CTUh	3.38E-12	6.13E-10	5.65E-10	1.18E-09	2.35E-09	172%
AC	mol H+ eq	7.01E-05	2.45E-03	6.10E-04	3.13E-03	1.95E-04	6.23%
EP	kg P eq	1.17E-05	3.98E-04	8.84E-05	4.98E-04	2.96E-04	62%
ETX	CTUe	2.00E-02	1.03E+00	1.33E+00	2.38E+00	7.15E+00	140%
WF	m^3 depriv.	2.95E-03	5.69E-02	9.08E-02	1.51E-01	1.83E+01	2060%
ADff	MJ	2.06E-01	6.54E+00	1.22E+00	7.97E+00	1.56E+00	20%
ADe	kg Sb eq	1.64E-07	6.24E-06	1.63E-06	8.03E-06	1.90E-06	23.80%
CED	MJ	4.79E-02	1.51E+00	2.74E-01	1.83E+00	3.40E-01	25%

Monte Carlo (n = 1,000) used triangular/log-normal parameterization for foreground energy and reagent use and Ecoinvent pedigree for background. For ETX/HTc/HTnc/WF, wider confidence intervals reflect method- and dataset-related variance (e.g., fate/exposure modelling, regional water factors). We report medians with 95% CIs and use these categories for qualitative interpretation; quantitative scenario decisions are based on more stable midpoints (CC, CED, AC, POF).

Table S13. Disaggregated Environmental Impacts (Base Case: L/S=5, -200 mA cm^{-2} and 1.5 M NaCl): Characterised values

Impact category	Unit	Electricity (milling)	Electricity (MWL)	HCl (MWL)	Waste (MWL)	Electricity (GDEx)	NaCl (GDEx)	CO_2 (GDEx)	Tap water (GDEx)	Waste anolyte (GDEx)	Waste supernatant (GDEx)	Cl_2/CO_2 air emission (GDEx)
CC	kg CO_2 eq	1.22E-02	3.31E-01	1.15E-01	1.13E-02	2.65E-02	2.14E-05	2.42E-03	3.63E-04	7.23E-03	7.19E-02	1.22E-03
OD	kg CFC11 eq	2.28E-10	6.17E-09	5.33E-09	3.09E-10	4.94E-10	2.05E-13	3.75E-11	5.38E-12	3.69E-10	3.65E-09	0.00E+00
POF	kg NMVOC eq	3.16E-05	8.55E-04	2.85E-04	9.90E-05	6.84E-05	9.28E-08	4.19E-06	1.17E-06	2.08E-05	2.14E-04	0.00E+00
PM	disease incidence	2.49E-10	6.74E-09	3.19E-09	1.49E-09	5.39E-10	1.57E-12	4.10E-11	2.24E-11	3.20E-10	3.28E-09	0.00E+00
HTnc	CTUh	1.90E-10	5.14E-09	1.48E-09	1.92E-10	4.11E-10	5.06E-13	9.81E-11	2.01E-11	1.03E-10	1.03E-09	0.00E+00
HTc	CTUh	3.38E-12	9.14E-11	5.18E-10	3.64E-12	7.31E-12	9.87E-15	7.41E-13	4.37E-13	5.16E-11	5.05E-10	0.00E+00
AC	mol H+ eq	7.01E-05	1.89E-03	4.65E-04	8.64E-05	1.51E-04	1.52E-07	6.40E-06	1.94E-06	4.09E-05	4.09E-04	0.00E+00
EP	kg P eq	1.17E-05	3.16E-04	7.26E-05	9.32E-06	2.53E-05	1.21E-08	7.02E-07	2.33E-07	5.68E-06	5.65E-05	0.00E+00
ETX	CTUe	2.00E-02	5.41E-01	4.47E-01	4.31E-02	4.33E-02	9.89E-05	3.31E-03	5.91E-04	6.66E-02	6.56E-01	5.63E-01
WF	m^3 depriv.	2.95E-03	7.98E-02	4.45E-02	-6.74E-02	6.38E-03	1.02E-05	4.49E-04	5.20E-02	3.60E-03	2.84E-02	0.00E+00
ADff	MJ	2.06E-01	5.56E+00	9.61E-01	1.46E-02	4.45E-01	1.42E-04	1.04E-02	4.42E-03	7.06E-02	6.93E-01	0.00E+00
ADe	kg Sb eq	1.64E-07	4.44E-06	1.77E-06	2.88E-08	3.55E-07	6.66E-10	2.78E-08	1.99E-09	1.15E-07	1.13E-06	0.00E+00
CED	MJ	4.79E-02	1.30E+00	2.12E-01	3.17E-03	1.04E-01	3.07E-05	2.33E-03	9.48E-04	1.55E-02	1.52E-01	0.00E+00

Table S14. Comparison of Environmental Impacts between Base Case and Alternative Scenarios: Characterised values

Impact category	**Unit**	**L/S=5, -200 mA cm^{-2} and NaCl**	**L/S=5, -40 mA cm^{-2} and NaCl**	**L/S=5, -200 mA cm^{-2} and Na_2SO_4**
CC	kg CO_2 eq	5.79E-01	5.77E-01	5.92E-01
OD	kg CFC11 eq	1.66E-08	1.64E-08	1.68E-08
POF	kg NMVOC eq	1.58E-03	1.55E-03	1.61E-03
PM	disease incidence	1.59E-08	1.57E-08	1.61E-08
HTnc	CTUh	8.65E-09	8.64E-09	8.86E-09
HTc	CTUh	1.18E-09	1.18E-09	1.19E-09
AC	mol H+ eq	3.13E-03	3.06E-03	3.20E-03
EP	kg P eq	4.98E-04	4.87E-04	5.10E-04
ETX	CTUe	2.38E+00	2.14E+00	1.84E+00
WF	m^3 depriv.	1.51E-01	1.48E-01	1.54E-01
ADff	MJ	7.97E+00	7.77E+00	8.19E+00
ADe	kg Sb eq	8.03E-06	7.91E-06	8.21E-06
CED	MJ	1.83E+00	1.79E+00	1.89E+00

4.5 Techno-Economic Assessment

The TEA considered a base treatment capacity of 50 L h^{-1} and an upscaled capacity of 100 L h^{-1}, together with additional economic scenarios addressing higher spent automotive catalyst cost and increased product selling price. The detailed CAPEX and OPEX assumptions for the 50 L h^{-1} and 100 L h^{-1} cases are provided in Tables S15–S18.

For GDEx, scale-up was treated by numbering-up cells/stacks to maintain the same charge input per treated volume at the selected current density. Each cell was assumed to provide 325 cm^2 of available electrode area, with a maximum of six cells per stack. Thus, the required number of cells was calculated as $\mathrm{N_{cells}} = \mathrm{A_{required}}/325$, with the result rounded up to ensure sufficient installed electrode area. The number of stacks was then calculated from the number of required cells and the maximum stack size: $\mathrm{N_{stacks}} = \mathrm{N_{cells}}/6$, again rounding up where needed. This gives 6 cells (1 stack) for 50 L h^{-1} and 11 cells (2 stacks) for 100 L h^{-1}. Stack costs include PTFE flow frames/channels, stainless-steel end plates, tie rods/compression hardware, and support stand; Pt-based anodes were included separately in CAPEX, while separators and gas-diffusion cathodes were treated as OPEX replacement items.

For MWAL, the number of reactors was calculated from the required MWAL treatment flowrate and the semi-batch cycle time. One filling-to-filling cycle was assumed to take approximately 8 min. With a filling volume of 1.2 L per reactor, this corresponds to an effective capacity of 9 L h^{-1} per reactor. The required number of MWAL reactors was therefore obtained from the ratio between the target MWAL flowrate ($\mathrm{Q_{MWAL}}$) and this per-reactor capacity: $\mathrm{N_{MWAL}} = \mathrm{Q_{MWAL}}/9$; with the result rounded up to ensure sufficient installed capacity. This gives 7 MWAL reactors for the 50 L h^{-1} case and 13 MWAL reactors for the 100 L h^{-1} case. In the integrated process, the MWAL flowrate used for sizing also accounts for internal stream recirculation and water losses.

Peripheral equipment such as pumps, filtration units, grinding/decanning units, sensors, and auxiliary components was assumed to be sufficiently overdesigned at the base scale to cover the 50–100 L h^{-1} range and was therefore not scaled proportionally. This is a simplifying assumption and is acknowledged as a TEA limitation. A Lang factor of 3, together with maintenance and safety/contingency factors, was applied to account for installation, indirect costs, and scale-up uncertainty. Detailed CAPEX assumptions are provided in Tables S15 and S17.

The spent automotive catalyst input was estimated from the target PGM throughput and the average PGM content per catalyst unit. Each unit was assumed to contain 1.5 kg of catalyst material with a total PGM concentration of 2915 mg kg^{-1}, corresponding to 4.37 g PGM per unit. The required number of catalyst units was therefore obtained by dividing the annual PGM demand by 4.37 g PGM $unit^{-1}$. For the 100 L h^{-1} scenario, this gives 117,427 units $year^{-1}$, equivalent to 513.45 kg PGM $year^{-1}$ and an annual feedstock cost of 20.30 M€ $year^{-1}$ at 172.84 € per unit. This corresponds to 22.24 kg h^{-1} of milled automotive catalyst entering MWAL and 29.76 kg h^{-1} of moisturised residue/waste after PGM removal. Detailed OPEX assumptions are provided in Tables S16 and S18.

Table S15. Capital Expenditure (CAPEX) breakdown for the 50 and 100 L h^{-1} scenarios.

Item	Cost (€/unit)	Base scenario: 50 L h^{-1}		Scenario: 100 L h^{-1}	
		Quantity	Total Cost (k€)	Quantity	Total Cost (k€)
IBC container	13,250	2	26.50	2	26.50
Fan + Chiller	15,500	1	15.50	1	15.50
Grinder	50,000	1	50.00	1	50.00
Decanning unit	15,000	1	15.00	1	15.00
MWAL reactors	14,286	7	100.00	13	185.71
Heat Exchanger	1,000	2	2.00	2	2.00
Filtration Unit MWAL	50,000	1	50.00	1	50.00
Power Supply	10,000	1	10.00	1	10.00
Electrochemical stack*	10,000	1 (6 unit cells)	10.00	2 (11 unit cells)	20.00
Pt/Ta anode**	973	3	2.92	6	5.838
Recirc. tanks (Anolyte & Catholyte)	500/5,000	1 each	5.50	1 each	5.50
UV-Vis Spectrophotometer	15,000	1	15.00	1	15.00
Turbidimeters	5,000	1	5.00	1	5.00
Settler	1000	2	2.00	2	2.00
Dryer	2,000	1	2.00	1	2.00
Pumps	5,000	12	60,00	12	60,00
Temperature Sensors	500	5	2.50	5	2.50
pH meters	3,000	3	9.00	3	9.00
Conductivity meters	3,000	2	6.00	2	6.00
Tanks	500	4	0.20	4	0.20
TOTAL CAPEX (before Lang factor and safety factor)	-	-	**390.92**		**499.55**

* Includes PTFE flow frames/channels, stainless steel end plates, tie-rods/compression hardware, and the support stand for a 6-unit cell stack. Pt-based anodes are considered separately as another entry in CAPEX, and separator and gas-diffusion cathodes are considered in the OPEX.

** Platinum-coated tantalum anodes with a geometric area of 325 cm^2 each. In the present stack layout, one anode is shared by two cells; therefore, three anodes are required for the 50 L h^{-1} case and six anodes for the 100 L h^{-1} case.

Table 16. Annual Operational Expenditure (OPEX) breakdown for the 50 and 100 L h^{-1} scenarios

Category	Item	Unit Cost (€)	Technical basis / assumptions	**Base scenario: 50 L h^{-1}**		**Scenario: 100 L h^{-1}**	
				Quantity/Usage	Annual Cost (k€ year^{-1})	Quantity/Usage	Annual Cost (k€ year^{-1})
Replacement	Membrane/diaphragm	500 per m^2	4 replacements year^{-1}	0.78 m^2 year^{-1}	0.39	1.43 m^2 year^{-1}	0.72
	Gas Diffusion Electrodes	3000 per m^2	4 replacements year^{-1}	0.78 m^2 year^{-1}	2.34	1.43 m^2 year^{-1}	4.29
	Tubing	500 per maintenance	5 replacements year^{-1}	-	2.50	-	2.50
Power	GDEx-Stack	200 per MWh	-	13.6 MWh year^{-1}	2.72	24.9 MWh year^{-1}	4.98
	Pumps (12 units)		-	2.6 MWh year^{-1}	0.52	5.2 MWh year^{-1}	1.04
	Grinding		0.09 kWh kg^{-1}	8,3 MWh year^{-1}	1.66	16.56 MWh year^{-1}	3.31
	Decanning		0.07 kWh kg^{-1}	6,2 MWh year^{-1}	1.23	12.33 MWh year^{-1}	2.47
	MWAL		0.72 kWh L^{-1}	222 MWh year^{-1}	44.39	444 MWh year^{-1}	88.76
MWAL Input	Spent automotive catalyst (AC)	172.84 per spent AC	1.5 kg monolith per spent AC unit	58,714 units_{AC} year^{-1}	10,147.71	117,427 units_{AC} year^{-1}	20,295.42
Chemicals	HCl	0.2 per L	Make-up/reacidification for 1.5 M HCl leaching medium	49,024 L year^{-1}	9.81	98,047 L year^{-1}	19.61
	NaCl	0.2 per kg	NaCl for anolyte	18,514 kg year^{-1}	3.70	37,028 kg year^{-1}	7.41
	CO_2	300 per ton (0.00147 per NL)	GDEx gas feed: 0.4 mL min^{-1} cm^{-2}	46.8 L h^{-1}	32.73	85.8 L h^{-1}	60.01
Water	Wash particles	0.0015 per L	500 L kg^{-1}	112,039 L year^{-1}	0.53	224,326 L year^{-1}	0.93
	Anolyte		40% of catholyte flow rate	158,400 L year^{-1}		316,800 L year^{-1}	
	Heat exchanger		Cooling-water: 10 L h^{-1}	79,200 L year^{-1}		79,200 L year^{-1}	
Personnel	Personnel Cost	58,500 per person year^{-1}	4 persons	4 persons	468.00	4 persons	468.00
Drying	Energy drying	200 per MWh	540 kcal kg^{-1} (80% humidity PGM NPs, 30% heat losses)	0.81 MWh year^{-1}	0.16	1.61 MWh year^{-1}	0.32
Waste management	Spent leachate	0.2 per L	PGM-depleted GDEx supernatant (bleed)	55,989 L year^{-1}	50.74	111,977 L year^{-1}	101.48
	Spent anolyte	0.1 per L	-	158,400 L year^{-1}		316,800 L year^{-1}	
	Moist PGM-depleted catalyst residue	0.2 per kg	Residue after filtration/washing	118,526 kg year^{-1}		237,051 kg year^{-1}	
TOTAL OPEX (Before Maintenance and Safety Factor)	-	-		-	**10,772.04**	-	**21,067.09**

Table S17. Adjusted CAPEX after application of Lang and safety factors for the 50 and 100 L h^{-1} scenarios.

Adjustment type	Factor	Value (M€)	
		Base scenario: 50 L h^{-1}	Scenario: 100 L h^{-1}
Lang Factor	3	1.17	1.50
Safety Factor	20%	0.23	0.30
TOTAL ADJUSTED CAPEX	-	**1.41**	**1.80**

Table S18. Adjusted OPEX after application of maintenance and safety factors for the 50 and 100 L h^{-1} scenarios.

Adjustment type	Factor	Value (M€ $year^{-1}$)	
		Base scenario: 50 L h^{-1}	Scenario: 100 L h^{-1}
General Maintenance	10% of OPEX (excluding spent automotive catalyst cost)	0.06	0.08
Safety Factor	20% of OPEX (accounting for maintenance)	2.17	4.23
TOTAL ADJUSTED OPEX	-	**13.00**	**25.35**

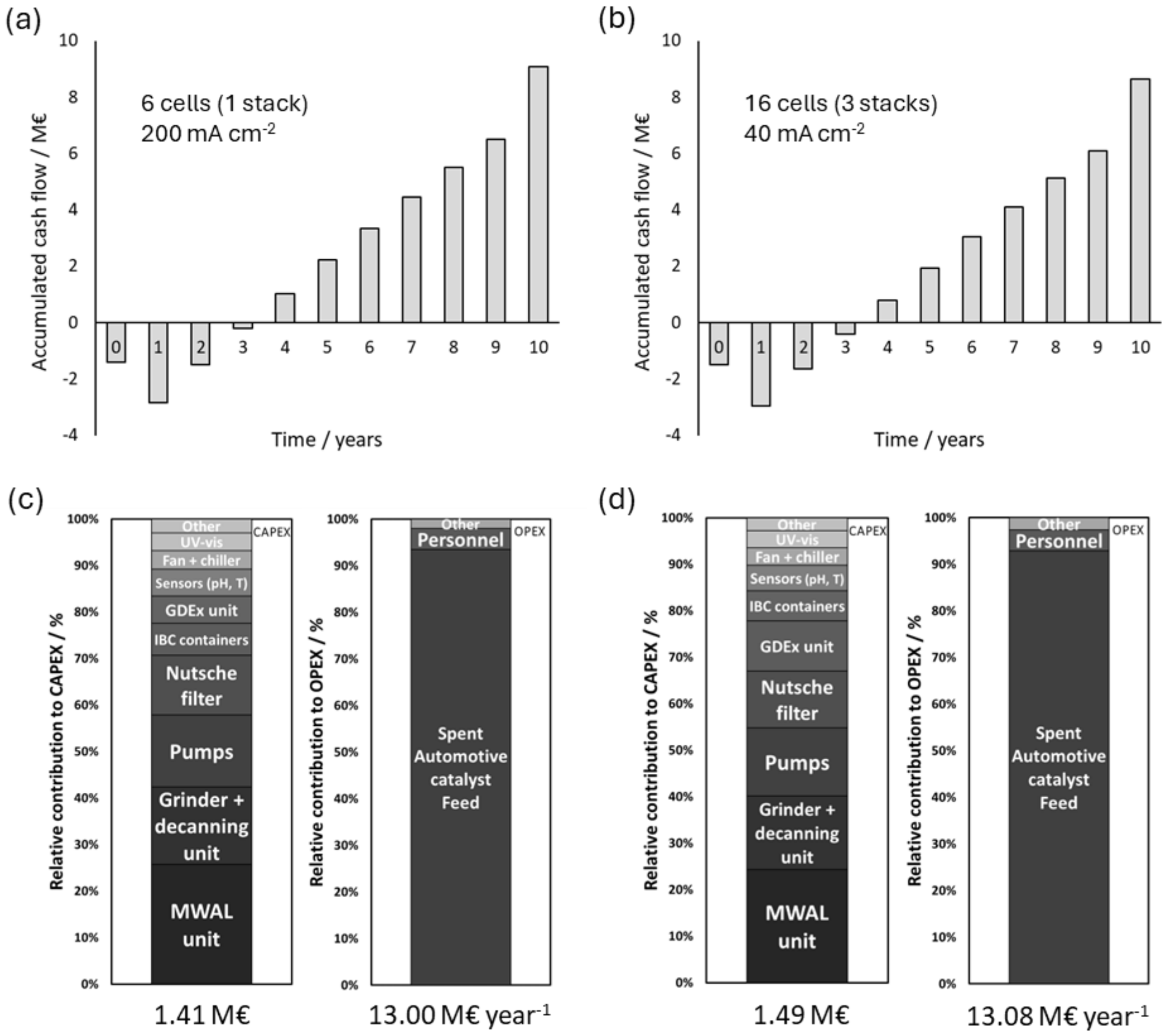

Figure S13. TEA results for different scale-up configurations at a treatment capacity of 50 L h^{-1}. (a) and (b) present the same accumulated cash flow results of the scenarios where 6 cells and 200 mA cm^{-2} current density or 16 cells and 40 mA cm^{-2} are used, respectively. (c) and (d) CAPEX and OPEX breakdown of the aforementioned scenarios.

Table S19. Summary of results from TEA analysis and assumptions considered for Net Present Value (NPV) calculation for the 50 L h^{-1} base scenario. Here, r denotes the discount rate and WACC the Weighted Average Cost of Capital.

Time horizon	10 years
CAPEX	1.41 M€
Working capital	20 % (of sales)
	1.88 M€
Revenues	15.08 M€/year
OPEX	13.00 M€/year
Depreciation (linear)	10 years
	141 k€/year
Tax rate	35 %
Inflation rate	3 %
Residual value	10 % (of CAPEX)
	141 k€
***r* = WACC**	7 %

Table S20. Year-by-year cash-flow schedule and discounted cash-flow (DCF) calculation for the NPV of the integrated MWAL–GDEx process over a 10-year horizon for the 50 $L\ h^{-1}$ base scenario. The assumptions used for the calculation are summarised in Table S19.

Years	0	1	2	3	4	5	6	7	8	9	10
CAPEX / k€	-1,407										141
Working capital / k€		-2,953									2,953
Invested Funds (IF) / k€	-1,407	-2,953									3,094
Sales (S) / k€		14,764	15,207	15,663	16,133	16,617	17,116	17,629	18,158	18,703	19,264
Costs (C) / k€		-11,784	-12,137	-12,501	-12,876	-13,263	-13,660	-14,070	-14,492	-14,927	-15,375
Depreciation / k€		-141	-141	-141	-141	-141	-141	-141	-141	-141	-141
Profit before taxes (PBT) / k€		2,981	3,070	3,162	3,257	3,355	3,455	3,559	3,666	3,776	3,889
Taxes (T) / k€		-1,043	-1,075	-1,107	-1,140	-1,174	-1,209	-1,246	-1,283	-1,322	-1,361
Profit after taxes (PAT)/ k€		1,937	1,996	2,055	2,117	2,181	2,246	2,313	2,383	2,454	2,528
Cash Earnings (CE) / k€		2,078	2,136	2,196	2,258	2,321	2,387	2,454	2,524	2,595	2,669
Cash flow / k€	-1,407	-875	2,136	2,196	2,258	2,321	2,387	2,454	2,524	2,595	5,762

Discounted cash flow (PV) / k€	-1,407	-817	1,866	1,793	1,722	1,655	1,590	1,528	1,469	1,411	2,929
Cumulative NPV / k€	-1,407	-2,225	-359	1,434	3,156	4,811	6,402	7,930	9,399	10,810	13,739